PHYSICAL REVIEW D **95,** 025023 (2017)

Direct-coupling lensing by antisymmetric tensor monopoles

Kamuela N. Lau* and Michael D. Seifert†

Department of Physics, Astronomy, and Geophysics, Connecticut College, 270 Mohegan Avenue, New London, Connecticut 06320, USA

(Received 30 September 2013; published 31 January 2017)

We discuss the effects of a direct coupling between a Lorentz-violating rank-two antisymmetric tensor field and the Maxwell field. Two possible couplings are considered, which can be distinguished by whether or not they lead to vacuum birefringence. In both cases, the magnitude of the field components and the coupling coefficient can be bounded by observational constraints. For light propagating in the presence of a topological defect solution, both couplings lead to the deflection of light rays; however, these angular deflections can be expected to be extremely small: 10^{-9} arcseconds for the nonbirefringent coupling, and no more than 10^{-26} arcseconds for the birefringent coupling. We discuss the plausibility of this phenomenon as a method for detection of these monopoles.

DOI: 10.1103/PhysRevD.95.025023

I. INTRODUCTION

Since its discovery and development at the beginning of the 20th century, Lorentz symmetry has been shown many times to be a very good symmetry of nature. Over the past decade and a half, however, there has been significant interest in investigating the possible ways in which Lorentz symmetry might be violated. One of the more active research programs being pursued to this end is the so-called Standard Model Extension, or SME [1]. This program "extends" the Standard Model by relaxing the requirement that the field combinations appearing in the Standard-Model Lagrangian be Lorentz scalars, and allowing combinations that are spacetime tensors to appear in the Lagrangian. Since the total action must still be a scalar, this means that the coefficients of these new terms will also be Lorentz tensors. The presence of these terms in the Lagrangian will affect the equations of motion of the fields (on the classical level) and the field propagators and Feynman rules (on the quantum level); in principle, then, these new tensor coefficients could be measured experimentally.[1] While none of these postulated coefficients has thus far been measured to be unambiguously nonzero, many bounds have been placed on the values of these coefficients, some of which are exceedingly stringent [2].

The SME was initially developed from a particle-physics perspective, and in particular, it was initially assumed that the "arena" in which fields exist and interact was flat Minkowski spacetime. In the context of flat spacetime, it is legitimate to assume that these new tensor coefficients are constants throughout space and time, and so can be viewed as "constants of nature." However, it was soon realized that this simple picture runs into trouble when we try to extend it to curved Riemannian spacetime. The first obvious objection in this case is that while many constant tensor fields exist on a flat manifold (e.g., $\partial_a A^b = 0$ has many solutions), a constant field (e.g., with $\nabla_a A^b = 0$) will not, in general, exist on a curved manifold. One might try to fix this problem by allowing the tensor coefficients of the new terms to be fixed nonconstant background tensor fields in the case of curved spacetime. However, this leads to a second problem with the original conception of the SME, less obvious but more serious. It was shown by Kostelecký [3] that the presence of a fixed background tensor field would necessarily lead to violations of the Bianchi identities. The only way to circumvent this problem, while retaining a spacetime that is well described by Riemannian geometry, is to allow these "background tensor fields" to be dynamic. Schematically, the full action of the theory will then be of the form

$$S = \int d^4x\sqrt{-g}[-(\nabla\mathcal{T})(\nabla\mathcal{T}) - V(\mathcal{T}) + \mathcal{L}_{\mathrm{SM}}(\Psi) + \mathcal{L}_{\mathrm{LV}}(\Psi,\mathcal{T})], \quad (1)$$

where $\mathcal{T}$ is a "Lorentz-violating" tensor field and Ψ represents the "conventional" matter fields of the Standard Model. In this Lagrangian, $\mathcal{L}_{\mathrm{SM}}$ is the Standard Model Lagrangian (including gravity), while $\mathcal{L}_{\mathrm{LV}}$ represents a small coupling between conventional matter and the Lorentz-violating tensor field. Since the Lorentz-violating tensor fields will now be dynamic, they will satisfy their own diffeomorphism-invariant equations of motion, and so

*knl1@alumni.williams.edu
†mseifer1@conncoll.edu

[1]Since these coefficients are tensors, their specification in terms of components is frame dependent; the standard choice of frame, and the one we will use for this paper, is the "Sun-centered frame," in which the z axis is parallel to the axis of the Earth's rotation and the x axis points towards the Vernal Equinox. Spherical angles in these coordinates are the standard astronomical right ascension and declination.

the Bianchi identities will automatically be satisfied so long as the equations of motion for this field (and the conventional matter fields) hold. By appropriately choosing the form of the potential $V(\mathcal{T})$, we can recover the "original SME" limit of flat spacetime and a constant background tensor field coupled to conventional matter. In such a picture, Lorentz symmetry is broken spontaneously rather than explicitly.

Since the Lorentz-violating tensor field $\mathcal{T}$ must be dynamical, it is natural to ask how this field will behave. The dynamics of such tensor fields in flat spacetime have been widely studied over the past few years, particularly in the case where $\mathcal{T}$ is a vector field A^a [4–7], a symmetric rank-two tensor field C^{ab} [8], or an antisymmetric rank-two tensor field B_{ab} [9]. Most of this prior work has centered on the situation where the tensor field is constant throughout space, taking on some value $\bar{\mathcal{T}}$ that minimizes its potential energy. However, this field value will not, generally speaking, be unique. A general potential $V(\mathcal{T})$ which breaks Lorentz symmetry will possess many possible values of $\mathcal{T}$ which minimize the potential energy; these field values form the so-called vacuum manifold in field space. This raises the possibility of topological defect solutions in the cases where the vacuum manifold is topologically nontrivial, and it has been shown that in the case of the antisymmetric rank-two tensor field, there exist topological monopole solutions [10,11]. These solutions are static, stable, and spherically symmetric, but the field is not in the vacuum manifold except asymptotically, and it approaches different points in the vacuum manifold as we go to spatial infinity in different directions. Moreover, if an antisymmetric tensor field capable of supporting these defects exists, one would expect a certain number of these monopoles to arise in the early Universe via the Kibble mechanism [12], and these monopoles might persist as relics today. In other words, not only are nonconstant tensor fields required in curved spacetimes, but they arise naturally in the context of (nearly) flat spacetime as well.

The possibility of a stable nonconstant background for a Lorentz-violating field leads us to ask what the effects of such a field on matter would be. To the best of our knowledge, all prior work dealing with Lorentz violation (particularly within the SME program [4–9]) has only dealt with position-independent effects; however, the existence of monopole solutions provides us with the motivation that position-dependent effects might also be physically relevant. In this paper, we examine the effects of an antisymmetric tensor monopole as a background field coupled to the electromagnetic field. In Sec. II, we present our model and review the formalism used to examine Lorentz-violating effects in electrodynamics. In Sec. III, we use observational and experimental data to gain an idea of the size of the effects which will arise and bound the parameters of our model. The main results of this work are then derived in Sec. IV, in which it is shown that an antisymmetric tensor monopole coupled directly to light would cause a lensing effect on light rays, akin to a gravitational lensing effect but in flat spacetime.

We will use units throughout where $\hbar = c = 1$. The metric signature will be $(-,+,+,+)$.

II. LORENTZ-VIOLATING ELECTRODYNAMICS

The main objects of interest in this paper are a conventional Maxwell field A_a and an antisymmetric rank-two tensor field B_{ab}. The Lagrangian for this model is

$$\mathcal{L} = -\frac{1}{4}F_{ab}F^{ab} - \frac{1}{6}F_{abc}F^{abc} - V(B_{ab}) - \frac{1}{4}(k_F)^{abcd}F_{ab}F_{cd}. \tag{2}$$

Taking each of these terms in turn, $F_{ab} = 2\partial_{[a}A_{b]}$ is the field strength for the Maxwell field, and $F_{abc} = 3\partial_{[a}B_{bc]}$ is the field strength for the "Lorentz-violating" field B_{ab}. The field B_{ab} has a potential energy $V(B_{ab})$, given by

$$V(B_{ab}) = \frac{\lambda}{4}(B_{ab}B^{ab} - b^2)^2, \tag{3}$$

where b is a characteristic mass scale for the field (having mass dimension 1), and λ is a dimensionless scaling constant for the potential. Finally, $(k_F)^{abcd}$ is a tensor that couples the Maxwell field to the Lorentz-violating field. We will examine specific forms for this tensor later; for the moment, we simply take this to be some general tensor depending on B_{ab}.

If we take the equations of motion associated with this Lagrangian, we obtain

$$\partial_b(F^{ba} + (k_F)^{bacd}F_{cd}) = 0 \tag{4}$$

for the Maxwell field A_a, and

$$\partial_c F^{cab} - \lambda(B_{cd}B^{cd} - b^2)B^{ab} - \frac{1}{4}\frac{\delta(k_F)^{cdef}}{\delta B_{ab}}F_{cd}F_{ef} = 0 \tag{5}$$

for the Lorentz-violating field B_{ab}. In particular, if we have $F_{ab} = 0$, the first equation of motion (4) is satisfied automatically, and the second equation of motion reduces to

$$\partial_c F^{cab} - \lambda(B_{cd}B^{cd} - b^2)B^{ab} = 0. \tag{6}$$

Given a solution to (6), we can then look for perturbational solutions about it, with "small" F_{ab}. Note that the terms in (5) involving F_{ab}, corresponding to the backreaction of the Maxwell field on the B_{ab} background, will be second order

in our "small" perturbation. The linearized versions of (4) and (5) are therefore decoupled, and we will hereafter ignore the linearized perturbations to the Lorentz-violating field B_{ab}.

To examine the dynamics of such perturbational solutions, we can employ the formalism of Kostelecký and Mewes [13]. For a general coupling tensor $(k_F)^{abcd}$, we can define a new antisymmetric tensor $\mathcal{D}^{ab}$ as

$$\mathcal{D}^{ab} = F^{ab} + (k_F)^{abcd}F_{cd}. \tag{7}$$

We can then suggestively denote the "electric" (time-space) and "magnetic" (space-space) parts of this tensor in terms of two spatial vector fields $\vec{D}$ and $\vec{H}$, such that $\mathcal{D}^{0i} = D^i$ and $\mathcal{D}^{ij} = \epsilon^{ijk}H^k$. In terms of these new objects, the full Maxwell equation (4) reduces to $\partial_b\mathcal{D}^{ba} = 0$; expressed in terms of the vectors $\vec{D}$ and $\vec{H}$, this reduces to

$$\vec{\nabla}\cdot\vec{D} = 0, \qquad \frac{\partial\vec{D}}{\partial t} - \vec{\nabla}\times\vec{H} = 0. \tag{8}$$

Moreover, since $\partial_{[a}F_{bc]} = 0$ by construction, we also have

$$\vec{\nabla}\cdot\vec{B} = 0, \qquad \vec{\nabla}\times\vec{E} + \frac{\partial\vec{B}}{\partial t} = 0. \tag{9}$$

Thus, the behavior of the Maxwell field in the presence of such a coupling is equivalent to its behavior in a linear medium; the tensor $\mathcal{D}^{ab}$ is the analog of the electric displacement tensor. The constitutive relations for this "medium" can be extracted from (7):

$$\begin{bmatrix}\vec{D}\\ \vec{H}\end{bmatrix} = \begin{bmatrix}\mathbf{1}+\kappa_{DE} & \kappa_{DB}\\ \kappa_{HE} & \mathbf{1}+\kappa_{HB}\end{bmatrix}\begin{bmatrix}\vec{E}\\ \vec{B}\end{bmatrix}, \tag{10}$$

where 1 is the 3×3 identity matrix and the κ's are 3×3 matrices given by

$$(\kappa_{DE})^{ij} = -2(k_F)^{0i0j}, \tag{11a}$$

$$(\kappa_{DB})^{ij} = -(\kappa_{HE})^{ji} = (k_F)^{0ikl}\epsilon^{jkl}, \quad \text{and} \tag{11b}$$

$$(\kappa_{HB})^{ij} = \frac{1}{2}\epsilon^{ikl}\epsilon^{jmn}(k_F)^{klmn}. \tag{11c}$$

Since the tensor $(k_F)^{abcd}$ is dependent on B_{ab}, the constitutive matrices (11) should also be expressible in terms of the components of B_{ab}. However, the precise relationship will depend on the form of $(k_F)^{abcd}$. We take the symmetry structure of this tensor to be the same as in Kostelecký and Mewes [13], namely, to have the same symmetry as the Riemann tensor with the additional constraint of a vanishing double trace $(k_F)_{ab}{}^{ab}$.[2] Under this assumption, it can be shown that it is impossible to construct a tensor $(k_F)^{abcd}$ out of the metric and B_{ab} that is linear in the Lorentz-violating field and that does not automatically vanish when contracted with $F_{ab}F_{cd}$. We must therefore consider couplings that are quadratic in B_{ab}. Careful examination of the possible tensor structures reveals two such possibilities: a "birefringent" coupling

$$(k_B)^{abcd} = \xi\left(B^{ab}B^{cd} - B^{[ab}B^{cd]} - \frac{1}{6}\eta^{a[c}\eta^{d]b}B_{ef}B^{ef}\right) \tag{12}$$

and a "monorefringent" coupling[3]

$$(k_M)^{abcd} = -\chi\left(B^{[a}{}_e\eta^{b][c}B^{d]e} + \frac{1}{4}\eta^{a[c}\eta^{d]b}B_{ef}B^{ef}\right). \tag{13}$$

(The reasons for these names will become clear below.) Since $(k_F)^{abcd}$ can be seen from (2) to be dimensionless, this implies that the coefficients ξ and χ in front of these terms will have mass dimension -2. These parameters are assumed to be "small" parameters that determine the strength of the coupling; we will assume them to be nonzero, but in principle, they could be either positive or negative.

We will examine each of these couplings in turn. In what follows, it will be helpful to define the spatial vectors $\vec{Q}$ and $\vec{R}$ to be the "electric" and "magnetic" parts of B^{ab}, respectively; in other words, $Q^i = B^{0i}$ and $R^i = \frac{1}{2}\epsilon^{ijk}B^{jk}$.

A. Birefringent coupling

Calculating the components of the constitutive tensors for the "birefringent" coupling (12), we find that

[2] In [13], the tensor $(k_F)^{abcd}$ is assumed to be constant. The symmetry structure chosen in that work was predicated on this assumption, as it implied that certain parts of this tensor did not affect the equations of motion. In the present work, we will eventually want to allow for nonconstant $(k_F)^{abcd}$; however, we have chosen to retain this symmetry structure in the present work so that the formalism in [13] still applies. Moreover, we suspect that the effects of these terms will be negligible for the purposes of this paper: the double trace term will correspond to a conformal rescaling of the metric, and so it will not affect light rays; and the completely antisymmetric term will be equivalent (via integration by parts) to a derivative of B_{ab}, which we will ultimately neglect in the optical limit.

[3] This coupling can be obtained by starting with the usual Maxwell term $\eta^{ac}\eta^{bd}F_{ab}F_{cd}$, replacing the "fiducial" metric η^{ab} with an "effective" metric $\tilde{\eta}^{ab} = \eta^{ab} + \chi B^a{}_c B^{bc}$, and discarding terms higher than first order in χ.

$$(\kappa_{DE})^{ij} = \xi\left[-2Q^iQ^j + \frac{1}{3}(\vec{Q}^2 - \vec{R}^2)\delta^{ij}\right], \tag{14a}$$

$$(\kappa_{DB})^{ij} = \xi\left[-2Q^iR^j + \frac{2}{3}(\vec{Q}\cdot\vec{R})\delta^{ij}\right], \quad \text{and} \tag{14b}$$

$$(\kappa_{HB})^{ij} = \xi\left[2R^iR^j + \frac{1}{3}(\vec{Q}^2 - \vec{R}^2)\delta^{ij}\right]. \tag{14c}$$

We can see immediately from (14) that the "linear medium" for our electromagnetic fields will be, in general, anisotropic; in fact, the only way for all of these matrices to be isotropic (i.e., proportional to δ^{ij}) is for all of them to vanish, with $\vec{Q} = \vec{R} = 0$.

These κ matrices can also be reparametrized in terms of certain parity-even and parity-odd combinations, denoted $\tilde{\kappa}_{e\pm}$, $\tilde{\kappa}_{o\pm}$, and $\tilde{\kappa}_{\rm tr}$ [13]; experimental bounds on the components of the tensor $(k_F)^{abcd}$ are usually quoted in terms of these matrices [2]. In our case, we have

$$(\tilde{\kappa}_{e\pm})^{ij} = \xi\left[-Q^iQ^j \pm R^iR^j + \frac{1}{3}(\vec{Q}^2 \mp \vec{R}^2)\delta^{ij}\right], \tag{15a}$$

$$(\tilde{\kappa}_{o+})^{ij} = 2\xi Q^{[i}R^{j]}, \tag{15b}$$

$$(\tilde{\kappa}_{o-})^{ij} = 2\xi\left[-Q^{(i}R^{j)} + \frac{1}{3}(\vec{Q}\cdot\vec{R})\delta^{ij}\right], \quad \text{and} \tag{15c}$$

$$\tilde{\kappa}_{\rm tr} = -\frac{\xi}{3}(\vec{Q}^2 + \vec{R}^2). \tag{15d}$$

It is known that if either $\tilde{\kappa}_{e+}$ or $\tilde{\kappa}_{o-}$ is nonzero, electromagnetic waves will experience vacuum birefringence at leading order in our Lorentz-violating parameter [13,14]. We can see from the form of (15) that a coupling of the form (12) will always produce birefringence unless both $\vec{Q}$ and $\vec{R}$ are zero.

Finally, since in all of the above expressions a change in the coupling strength ξ is indistinguishable from a rescaling of $\vec{Q}$ and $\vec{R}$, we will define two new vectors $\bar{Q} = \sqrt{|\xi|}\vec{Q}$ and $\bar{R} = \sqrt{|\xi|}\vec{R}$. In terms of these rescaled vectors, we have

$$(\tilde{\kappa}_{e\pm})^{ij} = \bar{\xi}\left[-\bar{Q}^i\bar{Q}^j \pm \bar{R}^i\bar{R}^j + \frac{1}{3}(\bar{Q}^2 \mp \bar{R}^2)\delta^{ij}\right], \tag{16a}$$

$$(\tilde{\kappa}_{o+})^{ij} = 2\bar{\xi}\bar{Q}^{[i}\bar{R}^{j]}, \tag{16b}$$

$$(\tilde{\kappa}_{o-})^{ij} = 2\bar{\xi}[-\bar{Q}^{(i}\bar{R}^{j)} + \frac{1}{3}(\bar{Q}\cdot\bar{R})\delta^{ij}], \quad \text{and} \tag{16c}$$

$$\tilde{\kappa}_{\rm tr} = -\frac{\bar{\xi}}{3}(\bar{Q}^2 + \bar{R}^2), \tag{16d}$$

where $\bar{\xi} = \xi/|\xi| = \pm 1$.

B. Monorefringent coupling

Applying the same techniques to the monorefringent coupling (13), we find that the constitutive matrices are somewhat simpler than in the previous case:

$$(\kappa_{DE})^{ij} = -(\kappa_{HB})^{ij} = -\frac{\chi}{2}(Q^iQ^j + R^iR^j), \quad \text{and} \tag{17a}$$

$$(\kappa_{DB})^{ij} = \chi Q^{[i}R^{j]}. \tag{17b}$$

As with the birefringent coupling, this "medium" can be seen to be anisotropic unless both $\vec{Q}$ and $\vec{R}$ vanish. However, this coupling does not produce birefringence: if we construct the matrices $\tilde{\kappa}_{e\pm}$, $\tilde{\kappa}_{o\pm}$, and $\tilde{\kappa}_{\rm tr}$ as above, we find that

$$(\tilde{\kappa}_{e-})^{ij} = -\frac{\chi}{2}\left[Q^iQ^j + R^iR^j - \frac{1}{3}\delta^{ij}(\vec{Q}^2 + \vec{R}^2)\right], \tag{18a}$$

$$(\tilde{\kappa}_{o+})^{ij} = \chi Q^{[i}R^{j]}, \tag{18b}$$

$$(\tilde{\kappa}_{e+})^{ij} = (\tilde{\kappa}_{o-})^{ij} = 0, \quad \text{and} \tag{18c}$$

$$\tilde{\kappa}_{\rm tr} = -\frac{\chi}{6}(\vec{Q}^2 + \vec{R}^2). \tag{18d}$$

The vanishing of $(\tilde{\kappa}_{e+})^{ij}$ and $(\tilde{\kappa}_{o-})^{ij}$ implies that to leading order in χ, there are no birefringent effects due to this coupling. This will have important implications for the experimental bounds we can place on the size of this coupling term.

Finally, we can define rescaled versions of the vectors $\vec{Q}$ and $\vec{R}$ as we did for the birefringent case, with $\bar{Q} = \sqrt{|\chi|}\vec{Q}$ and $\bar{R} = \sqrt{|\chi|}\vec{R}$. In terms of these, the nonzero matrices in (18) become

$$(\tilde{\kappa}_{e-})^{ij} = -\frac{\bar{\chi}}{2}\left[\bar{Q}^i\bar{Q}^j + \bar{R}^i\bar{R}^j - \frac{1}{3}\delta^{ij}(\bar{Q}^2 + \bar{R}^2)\right], \tag{19a}$$

$$(\tilde{\kappa}_{o+})^{ij} = \bar{\chi}\bar{Q}^{[i}\bar{R}^{j]}, \tag{19b}$$

$$\tilde{\kappa}_{\rm tr} = -\frac{\bar{\chi}}{6}(\bar{Q}^2 + \bar{R}^2). \tag{19c}$$

In parallel with the birefringent case, we have $\bar{\chi} = \pm 1$.

III. CONSTANT-FIELD PARAMETER BOUNDS

Up to this point, we have not made any particular assumptions concerning the properties of the "linear medium" in which our Maxwell fields are propagating; in particular, our constitutive relations (10) may well vary from point to point in space. In almost all of the literature on Lorentz symmetry violation to date, it is assumed that the Lorentz-violating fields form a constant background in

space. In such a circumstance, the constitutive relations (10) are the same at all points in space, and the Maxwell field behaves as though it is propagating in a homogeneous (though anisotropic) medium.[4] The monopole backgrounds that we will be examining in Sec. IV are nonconstant, and so some of the effects we will be examining do not have an analog in the current literature. However, we can still examine the behavior of our model in the case of a constant background field B_{ab} in order to get an idea of the size of the effects we are looking for.

A. Birefringent coupling bounds

As noted above, the coupling tensor (12) will necessarily lead to vacuum birefringence. Current observational bounds on vacuum birefringence are quite stringent; nonobservance of vacuum birefringence will thereby allow us to place tight bounds on the components $\bar{Q}^i$ and $\bar{R}^i$, which will in turn allow us to estimate the order of magnitude of the parameter combination $\sqrt{|\xi|}b$.

1. Bounds from optical and IR sources

The first major analysis of vacuum birefringence in the context of the SME was done by Kostelecký and Mewes [14]. Their analysis was able to place bounds on the magnitude of parameter σ (equal to twice the difference in the phase velocity between the two polarizations) for a list of sixteen optical and infrared sources, shown in Table I. This parameter σ_A for a given source A can in turn be expressed in terms of the components of the tensor $(k_F)^{abcd}$ and the right ascension and declination of the source $\{\alpha_A, \delta_A\}$. Putting all of these together, then, we see that each independent bound on σ_A will constrain some polynomial function of the $\bar{Q}^i$ and $\bar{R}^i$, and that this function will depend on the right ascension and declination of the source in question. The actual form of these functions is quite complicated, and the reader is referred to the Appendix for details on how they are constructed.

We treat each of these sixteen two-sided bounds in [14] as a strict exclusion; this leaves a small region of parameter space near the origin that is allowed under the simultaneous imposition of all of the bounds. The maximum magnitudes of the components $\bar{Q}^x$, $\bar{Q}^y$, and $\bar{Q}^z$ in this allowed region of parameter space are 1.56×10^{-16}, 1.54×10^{-16}, and 1.43×10^{-16}, respectively. The bounds on the magnitudes of $\bar{R}^x$, $\bar{R}^y$, and $\bar{R}^z$ are identical; this is to be expected, since all of the coefficients that control birefringent effects (i.e., the components of $\tilde{\kappa}_{e+}$ and $\tilde{\kappa}_{o-}$) are antisymmetric under the exchange $\vec{Q} \leftrightarrow \vec{R}$, and all of our observational bounds are taken to be symmetric about zero. Finally, the value of $\xi B_{ab}B^{ab} = 2\xi(-\vec{Q}^2 + \vec{R}^2)$ in the allowed region of parameter space is bounded by

$$|\xi B_{ab}B^{ab}| < 4.59 \times 10^{-32}. \tag{20}$$

This bound is symmetric about zero for the same reasons that the individual bounds on the components of $\bar{Q}$ and $\bar{R}$ are the same.

Finally, note that if the field is in the vacuum manifold, we will have $B_{ab}B^{ab} = b^2$. Since it will generally be the case that the vacuum manifold is in or near the vacuum manifold throughout the vast majority of space, we can equally well view the bound (20) as a constraint on the combination $|\xi|b^2$ of the model's parameters.

TABLE I. Sources used in the bounds placed in Sec. III A 1. Bounds on $|\sigma|$ are those from [14]; right ascension α and declination δ were found in the Centre de Donneés astronomiques de Strasbourg online catalog [15].

Source	α	δ	$\log_{10}\lvert\sigma\rvert$
IC 5063	$20^h52^m02^s$	$-57°04'08''$	−30.8
3A 0557 − 383	$05^h58^m02^s$	$-38°20'04''$	−31.2
IRAS 18325 − 5925	$18^h36^m58^s$	$-59°24'08''$	−31.0
IRAS 19850 − 1818	$20^h00^m52^s$	$-18°10'27''$	−31.0
3C 324	$15^h49^m49^s$	$21°25'39''$	−32.2
3C 256	$11^h20^m43^s$	$23°27'55''$	−32.2
3C 356	$17^h24^m19^s$	$50°57'40''$	−32.2
FIRST J084044.5+363328	$08^h40^m45^s$	$36°33'28''$	−32.2
FIRST J155633.8+351758	$15^h56^m34^s$	$35°17'57''$	−32.2
3CR 68.1	$02^h32^m29^s$	$34°23'46''$	−32.2
QSO J2359-1241	$23^h59^m54^s$	$-12°41'48''$	−31.1
3C 234	$10^h01^m50^s$	$28°47'09''$	−31.7
4C 40.36	$18^h10^m56^s$	$40°45'24''$	−32.2
4C 48.48	$19^h33^m05^s$	$48°11'42''$	−32.2
IAU 0211 − 122	$02^h14^m17^s$	$-11°58'45''$	−32.2
IAU 0828 + 193	$08^h30^m53^s$	$19°13'16''$	−32.2

2. Bounds from γ-ray sources

More recently, Kostelecký and Mewes published a work [16] based on six polarization measurements of gamma-ray bursts (Table II). The bounds on certain components of $(k_F)^{abcd}$ derived in this latter work were much more stringent than those from the work [14], by a factor of approximately 10^4.

The same analysis as in the previous subsection can be applied to this data. Within the allowed region of parameter space, the magnitudes of $\bar{Q}^x$, $\bar{Q}^y$, and $\bar{Q}^z$ are bounded by 1.12×10^{-18}, 1.00×10^{-18}, and 1.53×10^{-18}, respectively; as for the optical case, the bounds on $\bar{R}^x$, $\bar{R}^y$, and $\bar{R}^z$ are the same. Finally, the magnitude of $\xi B_{ab}B^{ab}$ is bounded by

[4] In fact, the bulk of the analysis in Kostelecký and Mewes' original papers [13,14] relies on this assumption. However, the definitions of theirs that we have presented in Sec. II do not rely on $(k_F)^{abcd}$ being constant in spacetime.

TABLE II. Gamma-ray sources used to place the bounds in Sec. III A 2. Redshift data given in [16] were converted to comoving distances L using the PLANCK 2015 data [17]; the bound on σ is then given by $\sigma < \pi/(2L\Delta E)$, where ΔE is the energy span of the gamma-ray burst.

Source	α	δ	z	$\log_{10}\lvert\sigma\rvert$
930131	182°	−8°	0.1	−35.7
960924	37°	3°	0.1	−35.7
041219A	6°	63°	0.02	−36.1
110301A	229°	29°	0.21	−36.5
110721A	333°	−39°	0.45	−36.8
100826A	279°	−22°	0.71	−37.0

$$|\xi B_{ab}B^{ab}| < 4.56 \times 10^{-36}. \tag{21}$$

While these bounds are significantly stronger, it should be noted that they are not as experimentally robust as the bounds derived from the optical and infrared observations in Sec. III A 1, particularly for this model. Since our parameter space is effectively six dimensional, and only six sources were used in the derivation of these newer bounds, we have "just enough" information to constrain all the parameters of our model. However, the method used to bound coefficients of $(k_F)^{abcd}$ in both [14,16] is based on the assumption that the light is not "accidentally" emitted in a normal mode, in which case the birefringent effects would be unobservable. If this were the case for any one of the six sources we have used, we would effectively "lose" this bound, which would likely leave at least one parameter of our model unconstrained. The larger number of data points used in the earlier work [14] leads to more robust constraints since the loss of one or two data points would still result in a bounded region of parameter space.

Finally, it must also be remembered for both the optical and infrared bounds and for the gamma-ray bounds that several of the sources used are at cosmological distances. The bounds in [13,14,16] assume that the tensor $(k_F)^{abcd}$ is effectively constant over the time of flight of the detected photons. However, if we are to take seriously the idea that the Lorentz-violating field B_{ab} has its own dynamics, it is entirely possible that this field [and therefore $(k_F)^{abcd}$] would evolve significantly over the time of flight of the photon. A more detailed model of the cosmological evolution of B_{ab} might lead to different bounds; however, such an investigation is well beyond the scope of this paper.

B. Monorefringent coupling bounds

As shown in Sec. II B, the coupling (13) does not result in birefringence; thus, we must look to other experimental constraints on the parameters for this coupling. The strongest bounds on the nonbirefringent coefficients of the SME are currently those from the cryogenic sapphire resonator experiments of Nagel *et al.* [18]. By carefully looking for "beat" frequencies in a pair of optical oscillators oriented at right angles, they were able to bound the difference in the speed of light between these two axes, and by changing the orientation and velocity of the apparatus (both actively and passively), they were able to look for the effects of various coefficients in the SME. A summary of their results is shown in Table III.

TABLE III. Bounds on the monorefringent coefficients of the minimal SME in the photon sector, as found by Nagel *et al.* [18].

Coefficient	Estimate and 1σ bound
$(\tilde{\kappa}_{e-})^{XY}$	$(-0.7 \pm 1.6) \times 10^{-18}$
$(\tilde{\kappa}_{e-})^{XZ}$	$(-5.5 \pm 4.0) \times 10^{-18}$
$(\tilde{\kappa}_{e-})^{YZ}$	$(-1.9 \pm 3.2) \times 10^{-18}$
$(\tilde{\kappa}_{e-})^{XX} - (\tilde{\kappa}_{e-})^{YY}$	$(-1.5 \pm 3.4) \times 10^{-18}$
$(\tilde{\kappa}_{e-})^{ZZ}$	$(-2.9 \pm 2.8) \times 10^{-16}$
$(\tilde{\kappa}_{o+})^{XY}$	$(-3.0 \pm 3.4) \times 10^{-14}$
$(\tilde{\kappa}_{o+})^{XZ}$	$(0.2 \pm 1.7) \times 10^{-14}$
$(\tilde{\kappa}_{o+})^{YZ}$	$(-2.0 \pm 1.6) \times 10^{-14}$
$\tilde{\kappa}_{\mathrm{tr}}$	$(-6.0 \pm 4.0) \times 10^{-10}$

We can use these experimental bounds to make a crude estimate of the bounds on the parameters in the monorefringent coupling case. We will consider the allowed region of parameter space to be bounded by the 2σ contour above and examine the bounds of this region.[5] Note that unlike in Sec. III A, these bounds are not symmetric about zero, so we must separately examine the $\bar{\chi} = +1$ and $\bar{\chi} = -1$ cases.

If we examine the resulting allowed region of parameter space, we find that the magnitudes of the components of $\bar{Q} = \sqrt{|\chi|}\vec{Q}$ and $\bar{R} = \sqrt{|\chi|}\vec{R}$ are all bounded by approximately 5×10^{-8}; the magnitude of the field norm $\chi B_{ab}B^{ab}$ in the allowed region of parameter space is bounded by

$$|\chi B_{ab}B^{ab}| < 5 \times 10^{-15}. \tag{22}$$

As with the birefringent case, this bound can also be viewed as a bound on the parameter combination $|\chi|b^2$.

IV. MONOPOLE LENSING

A. Geometric optics near a monopole

In the previous section, we worked under the assumption that the background field B_{ab} was constant in space and

[5]This is an extremely crude method of estimation and should only be trusted to within an order of magnitude. Beyond the obvious problems of treating the 2σ bounds as strict exclusions, it should also be noted that the SME coefficients in our model are strongly correlated: only six independent parameters determine the nine coefficients in Table III, while the analysis in [18] assumed that all of these coefficients were independent. A more sophisticated analysis, such as that in [7], would be necessary to place a more accurate bound.

time. However, recent work on monopole solutions [10,11,19] has shown that there exist spherically symmetric static solutions in which the field B_{ab} varies spatially, both in magnitude and direction. In the context of Lorentz-violating electrodynamics, this means that the κ-matrices appearing in the constitutive relations (10) vary from point to point in space (although not in time). In other words, in the presence of a monopole solution, electromagnetic fields act as though they were in an inhomogeneous, anisotropic, and possibly birefringent medium. In particular, the inhomogeneity of the medium implies that light rays traveling near the monopole will be deflected from straight-line paths.

To quantify this effect, we apply a geometric-optics approximation to the modified Maxwell equations (8) and (9). Our derivation will roughly follow the techniques of Sluijter *et al.* [20]. We choose an ansatz for the electromagnetic fields of the form

$$\vec{E}(t,\vec{x}) = \vec{e}(\vec{x})e^{ik(S(\vec{x})-t)}, \tag{23a}$$

$$\vec{B}(t,\vec{x}) = \vec{b}(\vec{x})e^{ik(S(\vec{x})-t)}. \tag{23b}$$

The constitutive relations (10) then imply that

$$\vec{D}(t,\vec{x}) = \vec{d}(\vec{x})e^{ik(S(\vec{x})-t)}, \tag{24a}$$

$$\vec{H}(t,\vec{x}) = \vec{h}(\vec{x})e^{ik(S(\vec{x})-t)}, \tag{24b}$$

where we have defined

$$\vec{d} = (\mathbf{1}+\kappa_{DE})\vec{e} + \kappa_{DB}\vec{b}, \tag{25}$$

$$\vec{h} = \kappa_{HE}\vec{e} + (\mathbf{1}+\kappa_{HB})\vec{b}. \tag{26}$$

[Recall that the κ's in these equations are 3×3 matrices acting on the vectors $\vec{e}(\vec{x})$ and $\vec{b}(\vec{x})$; moreover, we are now allowing these matrices to vary spatially, although not in time.] Plugging these into the modified Maxwell equations, we obtain the equations

$$\vec{\nabla}S\times\vec{h} + \vec{d} = -\frac{1}{ik}\vec{\nabla}\times\vec{h}, \tag{27a}$$

$$\vec{d}\cdot\vec{\nabla}S = -\frac{1}{ik}\vec{\nabla}\cdot\vec{d}, \tag{27b}$$

$$\vec{b}\cdot\vec{\nabla}S = -\frac{1}{ik}\vec{\nabla}\cdot\vec{b}, \tag{27c}$$

$$\vec{\nabla}S\times\vec{e} - \vec{b} = -\frac{1}{ik}\vec{\nabla}\times\vec{e}. \tag{27d}$$

We now apply the standard geometric-optics approximation and restrict our attention to solutions for which the length scale variations of the vectors $\vec{e}$, $\vec{b}$, $\vec{d}$, and $\vec{h}$ are much less than the length scale defined by k. In other words,

$$\left\{\frac{|\vec{\nabla}\vec{e}\,|}{|\vec{e}|}, \frac{|\vec{\nabla}\vec{b}\,|}{|\vec{b}|}, \frac{|\vec{\nabla}\vec{d}\,|}{|\vec{d}|}, \frac{|\vec{\nabla}\vec{h}\,|}{|\vec{h}|}\right\} \ll k \tag{28}$$

in some appropriate sense, which allows us to neglect the right-hand sides of the four equations (27). Note that if the background field B_{ab} is "slowly varying" in this sense, then the slow variation of $\vec{d}$ and $\vec{h}$ follows from the slow variation of $\vec{e}$ and $\vec{b}$. We will assume that we are working in a regime where B_{ab} is varying sufficiently slowly to make this approximation.

So far in this section, we have not assumed that the κ matrices have any particular form; our equations are valid for any (static) background field B_{ab}, assuming it is static and slowly varying. For the case of the monopole solution originally found in [10], the field configuration is of the form

$$B_{\theta\phi} = g(r)r^2\sin\theta, \tag{29}$$

with all other components vanishing. The function $g(r)$ is the solution to the differential equation[6]

$$\frac{\partial}{\partial r}\left(\frac{\partial g}{\partial r}+\frac{2}{r}g\right) - 2\lambda(2g^2-b^2)g = 0 \tag{30}$$

subject to the boundary conditions $g(0)=0$ and $g(\infty)=b/\sqrt{2}$. While a closed-form solution for $g(r)$ is not known, its asymptotic behavior as $r\to\infty$ is

$$g(r) = \frac{b}{\sqrt{2}}\left(1-\frac{1}{4\lambda b^2 r^2}-\frac{3}{8\lambda^2 b^4 r^4}+\cdots\right). \tag{31}$$

Finally, in terms of the "electric" and "magnetic" vectors $\vec{Q}$ and $\vec{R}$, it can easily be shown that for this solution we have $\vec{Q}=0$ and

$$\vec{R} = g(r)\hat{r}. \tag{32}$$

1. Birefringent coupling

At this point, we must focus on each coupling in turn. For the birefringent coupling (12), we see from Eq. (14) that the "off-diagonal" matrices κ_{DB} and κ_{HE} vanish, and that κ_{DE} becomes isotropic:

$$(\kappa_{DE})^{ij} = -\frac{1}{3}\xi g^2(r)\delta^{ij}, \tag{33}$$

[6]This equation is just the equation of motion for B_{ab} derived from the Lagrangian (2), under the imposition of the ansatz (29).

$$(\kappa_{HB})^{ij} = \xi g^2(r)\left(2\hat{r}^i\hat{r}^j - \frac{1}{3}\delta^{ij}\right). \tag{34}$$

This allows us to define effective permittivity and permeability tensors ϵ^{ij} and μ^{ij} such that $d^i = \epsilon^{ij}e^j$ and $b^i = \mu^{ij}h^j$. The permittivity tensor will be

$$\epsilon^{ij} = \delta^{ij} + (\kappa_{DE})^{ij} = \left(1 - \frac{1}{3}\xi g^2\right)\delta^{ij}, \tag{35}$$

while the inverse of the permeability tensor will be

$$\begin{aligned}(\mu^{-1})^{ij} &= \delta^{ij} + (\kappa_{HB})^{ij} \\ &= \left(1 - \frac{1}{3}\xi g^2\right)\delta^{ij} + 2\xi g^2\hat{r}^i\hat{r}^j.\end{aligned} \tag{36}$$

This last matrix can be inverted to yield

$$\mu^{ij} = \frac{1}{1 - \frac{1}{3}\xi g^2}\left[\delta^{ij} - \frac{2\xi g^2}{1 + \frac{5}{3}\xi g^2}\hat{r}^i\hat{r}^j\right]. \tag{37}$$

In the language of birefringent optics, then, the "medium" in which our waves are propagating will be electrically isotropic, magnetically anistropic, and unaxial; at all points, the "optical axis" of the medium will be the radial direction $\hat{r}$.

Combining all of the above, then, we have from (27a) and (25)

$$\vec{e} = -\frac{1}{\epsilon}(\vec{\nabla}S) \times \vec{h}, \tag{38}$$

where $\epsilon = 1 - \frac{1}{3}\xi g^2$ is the (position-dependent) permittivity. Plugging this into (27d), and defining the wave-normal vector $\vec{p} = \vec{\nabla}S$, we obtain

$$[p^i p^j - (\vec{p}\cdot\vec{p})\delta^{ij} + \epsilon\mu^{ij}]h^j = 0. \tag{39}$$

For a nontrivial wave amplitude $\vec{h}$ to exist, it must be the case that

$$\det[p^i p^j - p^2\delta^{ij} + \epsilon\mu^{ij}] = 0; \tag{40}$$

after some algebra, this condition boils down to

$$(p^2 - 1)\left(p^2 - \frac{\zeta_b}{1+\zeta_b}(\vec{p}\cdot\hat{r})^2 - \frac{1}{1+\zeta_b}\right) = 0, \tag{41}$$

where

$$\zeta_b = \frac{2\xi g^2}{1 - \frac{1}{3}\xi g^2} \approx 2\xi g^2 \tag{42}$$

to linear order in ξ.

For a given direction of $\hat{r}$ and value of ζ_b, Eq. (41) defines a surface in $\vec{p}$-space called the optical indicatrix. This surface consists of two ellipsoids which are tangent to each other at the points $\vec{p} = \pm\hat{r}$, and which do not otherwise intersect. These ellipsoids correspond to ordinary and extraordinary waves, respectively; the ordinary waves satisfy

$$\mathcal{H}_o = \frac{1}{2}(p_o^2 - 1) = 0, \tag{43}$$

while the extraordinary waves satisfy

$$\mathcal{H}_e = \frac{1}{2}((1+\zeta_b)p_e^2 - \zeta_b(\vec{p}_e\cdot\hat{r})^2 - 1) = 0. \tag{44}$$

(The reason for the choice of the overall factors in these equations will become clear in Sec. IV B.)

For the ordinary waves, requiring that $\vec{p}_o = \hat{p}_o$ is a unit vector causes Eq. (39) to reduce to

$$\left[\hat{p}_o^i\hat{p}_o^j - \frac{\zeta_b}{1+\zeta_b}\hat{r}^i\hat{r}^j\right]h_o^j = 0. \tag{45}$$

It is not hard to see that for this to be true, the vector $\vec{h}_o$ must be at right angles to both $\hat{p}_o$ and $\hat{r}$.[7] In other words, we can define the magnetic field direction $\hat{h}_o$ as

$$\hat{h}_o = \frac{\hat{p}_o \times \hat{r}}{|\hat{p}_o \times \hat{r}|}. \tag{46}$$

Equation (27a) then tells us that the (electric) polarization of the ordinary wave $\hat{e}_o$ is given by

$$\hat{e}_o = \frac{\hat{r} - \hat{p}_o(\hat{p}_o\cdot\hat{r})}{|\hat{r} - \hat{p}_o(\hat{p}_o\cdot\hat{r})|}. \tag{47}$$

In other words, the electric polarization for an ordinary wave points along the projection of $\hat{r}$ in the plane orthogonal to $\hat{p}_o$. These waves propagate at constant speed through space since p_o^2 is constant.

The polarization of the extraordinary waves is somewhat less obvious. We simply cite the work of [20], with the substitution $\vec{E} \leftrightarrow \vec{H}$.[8] The magnetic field direction $\hat{h}_e$ for an extraordinary wave with wave-front vector $\vec{p}_e$ can be shown to point in the direction

[7] In the case where $\hat{p}_o \| \hat{r}$, the wave direction is parallel to the optical axis, so the ordinary and extraordinary waves travel at the same speed.

[8] This substitution is necessary because [20] assumed the medium to be electrically anisotropic but magnetically isotropic. In the present case, however, our "medium" is electrically isotropic but magnetically anisotropic.

$$\hat{h}_e = \frac{(\vec{p}_e \times \hat{r}) \times [(1+\zeta_b)\vec{p}_e - \zeta_b(\vec{p}_e \cdot \hat{r})\hat{r}]}{|(\vec{p}_e \times \hat{r}) \times [(1+\zeta_b)\vec{p}_e - \zeta_b(\vec{p}_e \cdot \hat{r})\hat{r}]|}, \quad (48)$$

while the electric field vector $\hat{e}_e$ will point in the direction

$$\hat{e}_e = -\frac{\vec{p}_e \times \hat{r}}{|\vec{p}_e \times \hat{r}|}. \quad (49)$$

Note that the magnetic polarization direction $\hat{h}_e$ is not, in general, perpendicular to the extraordinary wave-front vector $\vec{p}_e$.

2. Monorefringent case

For the monorefringent coupling, the "on-diagonal" constitutive matrices (17) in the presence of a monopole become

$$(\kappa_{DE})^{ij} = -(\kappa_{HB})^{ij} = -\frac{\chi}{2} g^2(r)\hat{r}^i\hat{r}^j, \quad (50)$$

with the matrices κ_{DB} and κ_{HE} vanishing. Thus, we can define the permittivity and inverse permeability tensors as

$$\epsilon^{ij} = \delta^{ij} - \frac{1}{2}\chi g^2 \hat{r}^i\hat{r}^j, \quad (51)$$

$$(\mu^{-1})^{ij} = \delta^{ij} + \frac{1}{2}\chi g^2 \hat{r}^i\hat{r}^j. \quad (52)$$

In this case, we have a "medium" which is anisotropic both electrically and magnetically; once again, the "optical axis" of the medium will be the radial direction.

Following similar logic to the previous subsection, we can combine Eqs. (27a) and (27d) to yield the equation $M^{ij}e^j = 0$, where[9]

$$M^{ij} \equiv \epsilon^{ikm}\epsilon^{jln}(\mu^{-1})^{kl}p^m p^n - \epsilon^{ij}e^j = 0. \quad (53)$$

This implies that the determinant of M^{ij} must vanish; after some algebra, this condition reduces to

$$(p^2 - \zeta_m(\vec{p}\cdot\hat{r})^2 - (1-\zeta_m)) \times ((1+\zeta_m)p^2 - \zeta_m(\vec{p}\cdot\hat{r})^2 - 1) = 0, \quad (54)$$

where we have defined

$$\zeta_m = \frac{\chi}{2} g^2. \quad (55)$$

The form of this condition is somewhat surprising, as it seems to imply that our optical indicatrix again consists of two ellipsoids: either

$$\mathcal{H}_a = \frac{1}{2}\left(\frac{1}{1-\zeta_m}p^2 - \frac{\zeta_m}{1-\zeta_m}(\vec{p}\cdot\hat{r})^2 - 1\right) = 0$$

or

$$\mathcal{H}_b = \frac{1}{2}((1+\zeta_m)p^2 - \zeta_m(\vec{p}\cdot\hat{r})^2 - 1) = 0.$$

In the previous case, this double-valued solution for $\vec{p}$ was indicative of birefringence; here, this interpretation would seem to be at odds with our results from Sec. II B. However, we note that $\mathcal{H}_a$ and $\mathcal{H}_b$ are equal to each other to leading order in our Lorentz-violating parameter χ; this would therefore imply that birefringence does not enter at leading order in χ, which is consistent with our results from Sec. II B.[10] Moreover, these factors are also equal to the expression $\mathcal{H}_e$ (44) found for the extraordinary waves of the birefringent propagator in the previous section. In effect, to leading order in our Lorentz-violating parameter, light waves in the presence of a monopole will behave the same in the monorefringent case (for both polarizations) as will the extraordinary waves in the birefringent case.

B. Ray tracing

Since the optical indicatrix for both polarizations of light in the monorefringent case is of the same form as the indicatrix for the extraordinary waves in the birefringent case, we can restrict our attention to the birefringent case. The results for the monorefringent case will then be obtainable from those for the extraordinary rays in the birefringent case under the substitution $\xi \to \chi/4$. For notational simplicity, we will "drop the subscript" on ζ_b and ζ_m, differentiating between these two quantities only when necessary and generally referring to both as simply ζ.

To analyze the paths of the rays in the birefringent case, we follow the method of Sluijter *et al.* [20] and interpret the factors $\mathcal{H}_o$ and $\mathcal{H}_e$ as point-particle Hamiltonians, whose trajectories evolve with respect to some parameter τ. In other words, we expect that for both ordinary rays and extraordinary rays, their position $\vec{x}(\tau)$ and momentum $\vec{p}(\tau)$ will satisfy

[9] Alternately, we can obtain the equation

$$[\epsilon^{ikm}\epsilon^{jln}(\epsilon^{-1})^{kl}p^m p^n - \mu^{ij}]h^j = 0$$

whose form is more closely analogous to Eq. (39) found in the birefringent case. However, in that case, we had $\epsilon^{ij} \propto \delta^{ij}$, which allowed this equation to simplify further. Since the medium is electrically anisotropic in this case, this form is not so useful.

[10] The fact that the two factors in (54) are not *exactly* equal to each other may indicate that this model would exhibit birefringence at higher order; the Mewes-Kostelecký formalism in [13,14] is only guaranteed to be valid to first order in the Lorentz-violating parameter. Given the bounds on χb^2 found in Sec. III B, such effects would be exceedingly small, so we will not pursue this possibility here.

$$\frac{d\vec{x}}{d\tau} = \nabla_{\vec{p}}\mathcal{H} \quad \text{and} \quad \frac{d\vec{p}}{d\tau} = -\nabla_{\vec{x}}\mathcal{H}. \tag{56}$$

Under this interpretation, it is evident that the ordinary rays will travel in straight lines: the ordinary Hamiltonian $\mathcal{H}_o$ is simply that of a free particle, and we will have

$$\frac{d\vec{x}}{dt} = \vec{p} \quad \text{and} \quad \frac{d\vec{p}}{dt} = 0. \tag{57}$$

[The insertion of the extra factors of $\frac{1}{2}$ in Eqs. (43) and (44) was done to make these equations look "nice".] Thus, the velocity $\vec{v}_o$ of an ordinary ray is constant with respect to time. Its electric and magnetic polarization directions will also be constant along its path: since the velocity is parallel to the wave-normal direction $\hat{p}_o$, it can be seen from (46) and (47) that $\vec{v}_o$, $\hat{h}_o$, and $\hat{e}_o$ are always mutually orthogonal, with $\hat{h}_o$ perpendicular to the plane containing $\vec{v}_o$ and $\hat{r}$.

The paths of the extraordinary rays are less straightforward to find. It is illustrative to pass from the Hamiltonian formulation for the ray's motion to a Lagrangian formulation. This can be done by performing a Legendre transformation on $\mathcal{H}_e$:

$$\mathcal{L}_e(\vec{x}, \dot{\vec{x}}) = \vec{p}\cdot\dot{\vec{x}} - \mathcal{H}_e, \tag{58}$$

where $\vec{p}$ can be written as a function of $\dot{\vec{x}}$ by inverting the relation

$$\dot{\vec{x}} = \nabla_{\vec{p}}\mathcal{H}_e = (1+\zeta)\vec{p} - \zeta(\vec{p}\cdot\hat{r})\hat{r}. \tag{59}$$

[It can then be seen from (48), (49) and (59) that $\vec{v}_e$, $\hat{h}_e$, and $\hat{e}_e$ are mutually orthogonal, as is the case for the ordinary rays.] To perform this Legendre transform, we define an inverse metric tensor g^{ij} as

$$g^{ij} = (1+\zeta)\delta^{ij} - \zeta\hat{r}^i\hat{r}^j, \tag{60}$$

in terms of which we have

$$\mathcal{H}_e = \frac{1}{2}(g^{ij}p_i p_j - 1). \tag{61}$$

[The extra factors of $(1+\zeta_b)$ in (44) were chosen to make this inverse metric more tractable.] It can then be seen that $\dot{x}^i = g^{ij}p_j$; inverting this, we then have $p_i = g_{ij}\dot{x}^i$, where g_{ij} is the metric tensor itself:

$$g_{ij} = \frac{1}{1+\zeta}\delta_{ij} + \frac{\zeta}{1+\zeta}\hat{r}_i\hat{r}_j. \tag{62}$$

Performing the Legendre transformation on $\mathcal{H}_e$, then, we find an effective point-particle Lagrangian for the extraordinary rays:

$$\mathcal{L}_e = \frac{1}{2}(g_{ij}\dot{x}^i\dot{x}^j + 1), \tag{63}$$

or, in terms of the path of the particle in spherical coordinates $\{r(\tau), \theta(\tau), \phi(\tau)\}$,

$$\mathcal{L}_e = \frac{1}{2}\left[\dot{r}^2 + \frac{1}{1+\zeta}r^2(\dot{\theta}^2 + \sin^2\theta\dot{\phi}^2) + 1\right]. \tag{64}$$

This Lagrangian is independent of ϕ and t, implying that there are two constants of motion: the angular momentum in the z direction, given by

$$\ell = \frac{1}{1+\zeta}r^2\sin^2\theta\dot{\phi}, \tag{65}$$

and the "energy,"

$$E = \frac{1}{2}\left[\dot{r}^2 + \frac{1}{1+\zeta}r^2(\dot{\theta}^2 + \sin^2\theta\dot{\phi}^2) - 1\right] = 0. \tag{66}$$

Restricting our attention to the equatorial plane ($\theta = \frac{\pi}{2}$), we can write this as

$$\frac{1}{2}\left[\dot{r}^2 + (1+\zeta)\frac{\ell^2}{r^2} - 1\right] = 0. \tag{67}$$

The motion of an extraordinary ray in the presence of a Lorentz-violating monopole is therefore equivalent to the motion of a particle with unit mass and total energy $E = 0$ in an effective one-dimensional potential

$$V_{\text{eff}}(r) = \frac{\ell^2(1+\zeta)}{2r^2} - \frac{1}{2}. \tag{68}$$

We now calculate the trajectory of a ray originating far from the monopole and passing nearby it. Combining (65) and (67), we can write down a differential equation relating r and ϕ along the trajectory:

$$\frac{d\phi}{dr} = \frac{\dot{\phi}}{\dot{r}} = \pm\frac{\ell(1+\zeta)r^{-2}}{\sqrt{1-\ell^2(1+\zeta)r^{-2}}}. \tag{69}$$

The total angle of deflection $\Delta\phi$ of the light ray can then, in principle, be found by integrating (69) from $r = \infty$ to $r_{\min}$ [defined as the value of r for which $\dot{r} = 0$ in (67) above] and doubling the result. However, a closed-form analytic expression for $\Delta\phi$ cannot be found, for the simple reason that ζ is a function of r, due to its dependence on the field profile g; as noted above, we do not have a closed-form expression for $g(r)$.[11] We can, however, plug (31) into (42)

[11]Numerical integration techniques can also be pursued, and such investigations are ongoing. However, we would still expect the geometric-optics approximation to break down if the ray trajectory attained sufficiently small values of r; near the monopole core, the length scale of the field variation would presumably be shorter than the wavelength of the light waves being deflected.

[or (55)] to obtain a power series for ζ in powers of r^{-1}. Moreover, since ξb^2 (or χb^2) is expected to be many orders of magnitude less than one, we can safely discard any terms of $\mathcal{O}(b^4)$ or higher. All told, then, we have the approximation

$$\zeta_b = \xi b^2\left(1 - \frac{1}{2\lambda b^2 r^2}\right) + \mathcal{O}(\xi^2 b^4, r^{-4}) \tag{70}$$

(where we have now specialized to the birefringent case). Defining $\mu = \xi b^2$ and $\nu = (2\lambda b^2 \ell^2)^{-1}$, and substituting $u = \ell/r$, we can write our integral for $\Delta\phi$ as

$$\Delta\phi \approx \int_0^{u_{\max}} \frac{1 + \mu - \mu\nu u^2}{\sqrt{1 - (1+\mu)u^2 + \mu\nu u^4}}\, du \tag{71}$$

where $u_{\max} = \ell/r_{\min}$. This integral can be evaluated exactly in terms of complete elliptic integrals; the result is

$$\Delta\phi \approx \frac{1}{u_{\max}}[E(q) + qK(q)], \tag{72}$$

where $u_{\max}^2$ is the (smaller) positive root of the denominator of (71), i.e.,

$$u_{\max}^2 = \frac{1 + \mu - \sqrt{(1+\mu)^2 - 4\mu\nu}}{2\mu\nu},$$

and $q = (1+\mu)u_{\max} - 1$. To linear order in μ and ν, we have $u_{\max}^{-1} \approx 1 + \mu/2 - \mu\nu/2$ and $q \approx \mu\nu$; thus, in this limit the angle swept out by the light ray becomes

$$\Delta\phi \approx \frac{\pi}{2}\left(1 + \frac{\mu}{2} + \frac{\mu\nu}{4}\right). \tag{73}$$

The deflection angle α between the propagation direction of the incoming ray and the outgoing ray will then be

$$\alpha = 2\Delta\phi - \pi \approx \frac{\pi}{2}\xi b^2\left(1 + \frac{1}{4\lambda b^2 \ell^2}\right), \tag{74}$$

where a positive value of α corresponds to a ray being attracted towards the monopole, and a negative value corresponds to a ray being repelled from the monopole. Note that the sign of α is the same as the sign of ξ; the quantity in parentheses must be assumed to be positive since the quantity $\nu = (2\lambda b^2 \ell^2)^{-1}$ has been assumed to be small.

It is instructive to ask what the meaning of the parameter ν is in the above calculation. To interpret it, we must assign some meaning to the constant of motion ℓ; the most illuminating way to do this is to relate it to the impact parameter β of the ray. The asymptotic velocity of the ray (at $r \to \infty$) can be seen from (67) to be $\dot{r} = \pm 1$; the plus or minus corresponds to infalling or outgoing rays. It can also be shown geometrically that a particle at location $(x, y, 0)$ with velocity $(-v, 0, 0)$ will have $\dot{\phi} = yv/r^2$. Thus, the quantity ℓ defined in (65) will be, for this particle,

$$\ell = \frac{1}{1+\zeta} yv. \tag{75}$$

In the limit $x \to \infty$ with y fixed, we can identify y with the impact parameter β for this trajectory; thus,

$$\ell = \frac{1 - \frac{1}{6}\xi b^2}{1 + \frac{5}{6}\xi b^2}\beta \approx (1 - \xi b^2)\beta, \tag{76}$$

where the prefactor comes from taking the limit of ζ as $r \to \infty$.

We see that ℓ is not exactly equal to the impact parameter β; however, since our result for the angular deflection (74) is only accurate to $\mathcal{O}(\xi^2 b^4)$, we can effectively replace ℓ with the impact parameter in this equation:

$$\alpha = 2\Delta\phi - \pi \approx \frac{\pi}{2}\xi b^2\left(1 + \frac{1}{4\lambda b^2 \beta^2}\right). \tag{77}$$

Note, meanwhile, that the characteristic length scale of the monopole core (as found in [10]) is $r_M = (\sqrt{\lambda} b)^{-1}$. Thus, we have $\nu = \frac{1}{2}(r_M/\beta)^2$; in other words, ν is best thought of as telling us about the ratio of the physical size of the monopole to the impact parameter of the ray.

Finally, recall that all of the above results hold for light rays of any polarization in the presence of a monorefringent coupling, under the substitution $\xi \to \chi/4$. In particular, a positive value of χ in (13) leads to light being "attracted" to the monopole, while a negative value will lead to light being "repelled." [The leading negative sign in (13) was chosen to yield this parallel interpretation.]

V. DISCUSSION

We have shown that a coupling between the Maxwell field and an antisymmetric rank-two tensor field B_{ab} can have effects on the propagation speed of light. These effects are dependent on the local magnitude of the field; this implies that light rays propagating through a nonuniform background, such as a monopole solution, will be deflected. For the "birefringent" coupling (12), light rays whose electric polarization vector lies in the scattering plane ("ordinary rays") will travel past the monopole undeflected; those whose electric polarization is perpendicular to the scattering plane, meanwhile ("extraordinary rays"), will be deflected due to their varying speed of

light. For the "monorefringent" coupling (13), all rays will be deflected regardless of their polarization. The leading-order angular deflection of the rays, in terms of the model's parameters ξ, λ, and b and the ray's impact parameter β, is given in (77) for the extraordinary rays in the birefringent case; the deflection for the monorefringent case is the same under the substitution $\xi \to \chi/4$.

It is important to note that the observed effects, while due to local anisotropies along the trajectory of the light ray, are not themselves anisotropic when projected onto the sky; the observed angular deflection pattern of distant sources is rotationally symmetric about the monopole's location on the sky. This is because the monopole itself is rotationally symmetric about this axis, so its lensing effects, when integrated along the line of sight, are also rotationally symmetric. This is to be contrasted with, for example, the work of Tso and Bailey [21]. In that work, the metric perturbations h^{ab} due to a compact object are distorted by a coupling to a constant background tensor $\bar{s}^{ab}$. In general, this causes the gravitational well to become asymmetric with respect to rotations, and the asymmetry of the gravitational well leads to a lensing pattern that is not rotationally symmetric on the sky.

In this respect, these effects are most similar to the gravitational lensing effects derived in previous work on the Lorentz-violating monopole solutions [10,11,19]. In the work of Li *et al.* [19], the gravitational deflection of a null ray due to a Lorentz-violating monopole solution is shown to be

$$\alpha_G = \frac{3}{2}\pi\epsilon - \frac{\sqrt{\epsilon}}{\sqrt{\lambda}br_m} + \frac{\epsilon}{20\lambda b^2 r_m^2} + \mathcal{O}(r_m^3), \qquad (78)$$

where $\epsilon = 16\pi G b^2$ and r_m is the radial coordinate of closest approach for the null ray in question. The most notable similarity between the gravitational deflection α_G and the direct-coupling deflection α is that, in both cases, the deflection angle does not vanish in the limit of large impact parameter. (This is to be contrasted with the case of light deflection by a conventional Schwarzschild metric, for which the deflection angle goes to zero as the impact parameter gets large.) In our case, we have

$$\alpha_\infty \equiv \lim_{\beta\to\infty}\alpha = \frac{\pi}{2}\xi b^2; \qquad (79)$$

the corresponding quantity in the gravitational case is $(\alpha_G)_\infty = \frac{3}{2}\pi\epsilon$. In this asymptotic limit, light rays behave as though there was a conical deficit angle due to the monopole.

However, this observation also illuminates an important difference between the direct-coupling case and the gravitational case. As noted previously, the coupling parameters ξ and χ can be either positive or negative. From (74), this implies that extraordinary rays in the birefringent coupling case are attracted towards the monopole when $\xi > 0$ but are repelled by it when $\xi < 0$. In the limit $\beta \to \infty$, the deflected rays behave as if in a space with a conical deficit angle when ξ is positive and a "conical surplus angle" when ξ is negative. In contrast, light rays are always deflected towards a monopole solution by its gravitational influence since ϵ [and therefore α_G, in the regime where (78) is valid] is always positive.

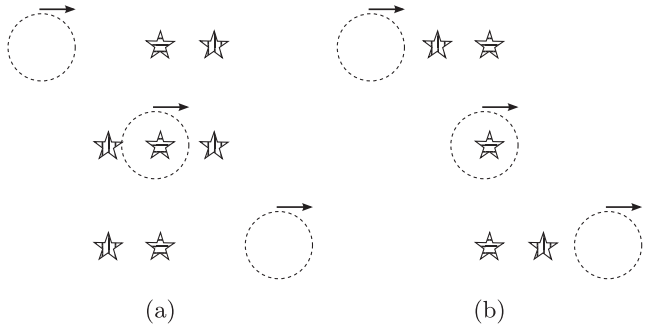

FIG. 1. Multiple images of a distant star created by a passing monopole, assuming a birefringent coupling with (a) $\xi > 0$ and (b) $\xi < 0$. The monopole's location is indicated by the dashed circle; the (electric) polarization of the light from each image is indicated by the direction of its stripes. For a monorefringent coupling, the horizontally polarized images would vanish, and the vertically polarized images would become unpolarized.

We can also ask what we would see if a monopole lay between us and a distant star. The effects are easiest to visualize in the birefringent case. For simplicity, consider the case in which the ray trajectory stays far from the monopole, so the approximation $\nu \approx 0$ is valid. It will always be the case that the ordinary rays sent out by the star will reach us along a straight-line path; the image observed this way would be highly polarized but otherwise undistorted. (This image would effectively serve as a "marker" of what we would see in the absence of the monopole.) However, the extraordinary rays would form zero, one, or two images, depending on the sign of ξ and the angular separation between the monopole and the distant star on the sky. A schematic illustration of the images of a distant star created by a passing monopole is shown in Fig. 1.

The fact that the extraordinary rays can create two (or zero) distinct images when the monopole, observer, and source are sufficiently closely aligned is characteristic of the conical deficit (or surplus) angle "seen" by the extraordinary rays, as mentioned above. If we approximate $\alpha \approx \alpha_\infty$ in Fig. 2 (i.e., ignoring the variation of α with impact parameter), we can see that an extraordinary ray can always get to the observer on the "same side" of the monopole as the ordinary rays (the right-hand side of the monopole in Fig. 2). Moreover, it can also get to the observer via the "opposite side" of the monopole, so long as the distance γD_S is less than $\alpha_\infty D_{MS}$. At this threshold

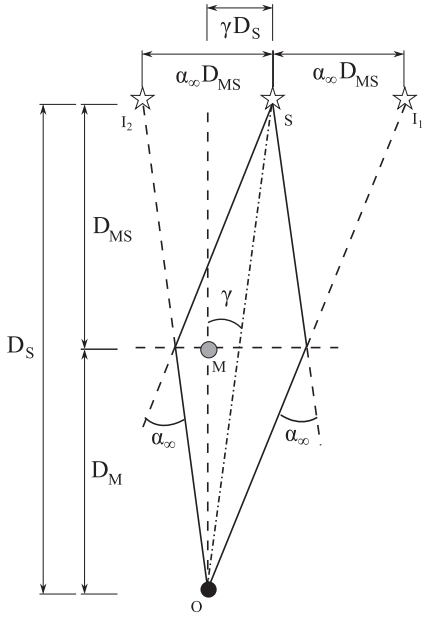

FIG. 2. Lensing diagram for triple image formation in the thin-lens approximation, assuming an attractive birefringent coupling. The points O, M, and S denote the observer, monopole, and source, respectively; I_1 and I_2 are the extraordinary images on the sky. Solid lines denote the paths of extraordinary rays from the source to the observer; the dashed-dotted line denotes the path of the ordinary rays.

and in this approximation, the ray would "skim" the opposite side of the monopole and then arrive at the observer from the direction of the monopole itself. (Of course, this limit would correspond to $\beta \to 0$ and therefore $\nu \to \infty$, before which point the above approximation for α would fail. Figure 2 should just be taken to be indicative of the range in which multiple extraordinary images can form.)

Of particular note is that there is *always* a double image of the star due to the birefringent effects of the monopole; the angular separation of the ordinary image and extraordinary image (in the limit $\nu \to 0$) will be

$$\theta_E = \frac{\alpha_\infty D_{MS}}{D_S} = \frac{\pi}{2}\xi b^2 \frac{D_{MS}}{D_S}, \tag{80}$$

where D_{MS} is the distance to the source from the monopole and D_S is the distance to the star.[12] Given the nonobservation of such double images on the sky, we can immediately say that if ξb^2 is nonzero, it must be sufficiently small that these double images are not observed. If we take the maximum angular resolution of the Very Long Baseline Array (about 120 μas [22]) as the best achievable resolution with current technology, we must thereby conclude that $|\xi b^2| < 10^{-10}$ or so. This bound is, of course, over 20 orders of magnitude less stringent than the bounds placed on ξb^2 via direct polarimetry measurements (see Sec. III A). We therefore conclude that these multiple images will, in general, be so closely spaced as to be unresolvable.[13]

Most of the above discussion carries over to the monorefringent coupling case as well; the only major difference is that both polarizations are deflected, rather than just one. This would mean that the horizontally polarized images in Fig. 1 would be superimposed on the vertically polarized images. In other words, for $\chi > 0$ we would initially see one unpolarized image; a second unpolarized image would then form to the left of the original, and finally the original image would vanish. The situation would be similar for $\chi < 0$, except that the original image would vanish *before* the appearance of the second image. The angular distance between these two images would be twice the angular scale calculated in (80) (under the substitution $\xi \to \chi/4$). Even though the bounds on the monorefringent coupling are much less stringent than the corresponding birefringent bounds (see Sec. III B), the angular resolution needed to resolve these distinct images is still 5 orders of magnitude greater than is feasible with current or near-future technology.

We can conclude that direct resolution of distinct images, while, in principle, possible, is quite implausible in practice; a monopole sitting at rest between the Earth and a distant source would therefore be effectively unobservable. However, the effects of this coupling could also be observable via intensity variations of the starlight due to a monopole in motion, passing between us and a distant source. With sufficiently close alignment of the source, monopole, and observer, one could hope to observe a sudden jump or drop in the received intensity of a distant source due to the appearance and disappearance of the aforementioned multiple images. Moreover, even without such good alignment, the bending of the rays would lead to a "focusing" or "defocusing" of the source's light rays as the monopole moves past, just as a compact gravitational object can focus such rays. These microlensing events would therefore cause smooth intensity variation of the distant source. Such variations of the source intensity (via the appearance of multiple images or, more likely, microlensing) are likely to be the only way that such monopoles could be observable via foreseeable technology. We are currently investigating these possibilities.

[12]This can be seen from the triangle formed by O, S, and I_1 (or I_2) in Fig. 2. It is also worth noting that the angle θ_E would be the radius of the "Einstein ring" in the case of perfect alignment between Earth, the monopole, and the distant star.

[13]When completed, the Event Horizon Telescope [23] will achieve an angular resolution an order of magnitude better than the Very Long Baseline Array—a substantial accomplishment, but still insufficient to observe these effects.

ACKNOWLEDGMENTS

A significant portion of this work was done during the authors' time at Williams College, and their support during this period is gratefully acknowledged. M. S. would also like to thank Matthew Mewes and Brett Altschul for helpful discussions during the preparation of this work.

APPENDIX: DEPENDENCE OF σ ON MODEL PARAMETERS

Following the language of [13], the parameter σ for a source with right ascension α and declination δ is given by

$$\sigma^2 = (\vec{\varsigma}_a \cdot \vec{k})^2 + (\vec{\varsigma}_c \cdot \vec{k})^2, \tag{A1}$$

where we have defined the three ten-dimensional vectors in this equation as

$$\varsigma_s^a = \begin{bmatrix} \cos^2\delta + \cos^2\alpha - \sin^2\alpha\,\sin^2\delta \\ \sin^2\delta\,\cos^2\alpha - \cos^2\delta - \sin^2\alpha \\ -2\sin\delta\,\sin\alpha\,\cos\alpha \\ -\sin\delta\,\sin\alpha\,\cos\alpha \\ \sin\delta(\sin^2\alpha - \cos^2\alpha) \\ -\cos\delta\,\sin\alpha \\ \cos\delta\,\cos\alpha \\ -\sin\delta\,\cos\delta\,\cos\alpha \\ -\cos^2\delta\,\sin\alpha\,\cos\alpha \\ -\sin\delta\,\cos\delta\,\sin\alpha \end{bmatrix}, \tag{A2}$$

$$\varsigma_c^a = \begin{bmatrix} -2\sin\delta\,\sin\alpha\,\cos\alpha \\ -2\sin\delta\,\sin\alpha\,\cos\alpha \\ \frac{1}{2}(1+\sin^2\delta)(\sin^2\alpha - \cos^2\alpha) \\ \frac{1}{2}(\sin\delta + \sin^2\alpha - \sin^2\delta\cos^2\alpha) \\ (1+\sin^2\delta)\sin\alpha\,\cos\alpha \\ -\sin\delta\,\cos\delta\,\cos\alpha \\ -\sin\delta\,\cos\delta\,\sin\alpha \\ \cos\delta\,\sin\alpha \\ \sin\delta(\sin^2\alpha - \cos^2\alpha) \\ -\cos\delta\,\cos\alpha \end{bmatrix}, \tag{A3}$$

and

$$k^a = \begin{bmatrix} -\bar{Q}^y\bar{R}^y + \frac{1}{3}\bar{Q}\cdot\bar{R} \\ \bar{Q}^x\bar{R}^x - \frac{1}{3}\bar{Q}\cdot\bar{R} \\ (\bar{Q}^y)^2 - (\bar{R}^y)^2 - \frac{1}{3}(\bar{Q}^2 - \bar{R}^2) \\ (\bar{Q}^z)^2 - (\bar{R}^z)^2 - \frac{1}{3}(\bar{Q}^2 - \bar{R}^2) \\ \bar{Q}^x\bar{Q}^y - \bar{R}^x\bar{R}^y \\ \bar{Q}^x\bar{Q}^z - \bar{R}^x\bar{R}^z \\ \bar{Q}^y\bar{Q}^z - \bar{R}^y\bar{R}^z \\ \bar{Q}^x\bar{R}^z + \bar{Q}^z\bar{R}^x \\ -\bar{Q}^x\bar{R}^y - \bar{Q}^y\bar{R}^x \\ \bar{Q}^y\bar{R}^z + \bar{Q}^z\bar{R}^y \end{bmatrix}. \tag{A4}$$

Note that this last vector contains the ten independent parameters of the matrices $\tilde{\kappa}_{e+}$ and $\tilde{\kappa}_{o-}$.

[1] D. Colladay and V. A. Kostelecký, Phys. Rev. D **58**, 116002 (1998).
[2] V. A. Kostelecky and N. Russell, Rev. Mod. Phys. **83**, 11 (2011).
[3] V. A. Kostelecký, Phys. Rev. D **69**, 105009 (2004).
[4] R. Bluhm and V. A. Kostelecký, Phys. Rev. D **71**, 065008 (2005).
[5] R. Bluhm, S.-H. Fung, and V. A. Kostelecký, Phys. Rev. D **77**, 065020 (2008).
[6] M. D. Seifert, Phys. Rev. D **79**, 124012 (2009).
[7] M. D. Seifert, Phys. Rev. D **81**, 065010 (2010).
[8] V. A. Kostelecký and R. Potting, Phys. Rev. D **79**, 065018 (2009).
[9] B. Altschul, Q. G. Bailey, and V. A. Kostelecký, Phys. Rev. D **81**, 065028 (2010).
[10] M. D. Seifert, Phys. Rev. Lett. **105**, 201601 (2010).
[11] M. D. Seifert, Phys. Rev. D **82**, 125015 (2010).
[12] T. Kibble, J. Phys. A **9**, 1387 (1976).
[13] V. A. Kostelecký and M. Mewes, Phys. Rev. D **66**, 056005 (2002).
[14] V. A. Kostelecký and M. Mewes, Phys. Rev. Lett. **87**, 251304 (2001).
[15] http://cdsweb.u-strasbg.fr/.
[16] V. A. Kostelecký and M. Mewes, Phys. Rev. Lett. **110**, 201601 (2013).
[17] Planck Collaboration, Astron. Astrophys. **594**, A13 (2016).
[18] M. Nagel, S. R. Parker, E. V. Kovalchuk, P. L. Stanwix, J. G. Hartnett, E. N. Ivanov, A. Peters, and M. E. Tobar, Nat. Commun. **6**, 8174 (2015).
[19] X.-Z. Li, P. Xi, and Q. Zhang, Phys. Rev. D **85**, 085030 (2012).
[20] M. Sluijter, D. K. G. de Boer, and J. J. M. Braat, J. Opt. Soc. Am. A **25**, 1260 (2008).
[21] R. Tso and Q. G. Bailey, Phys. Rev. D **84**, 085025 (2011).
[22] VLBA Observational Status Summary 2016B, Technical Report, National Radio Astronomy Observatory (2016).
[23] S. Doeleman, in *Proceedings of the "10th European VLBI Network Symposium and EVN Users Meeting", Manchester, UK* (2010), p. 053.